

# Forest Guided Smoothing

Isabella Verdinelli and Larry Wasserman  
Department of Statistics and Data Science  
Carnegie Mellon University

March 8 2021

## Abstract

We use the output of a random forest to define a family of local smoothers with spatially adaptive bandwidth matrices. The smoother inherits the flexibility of the original forest but, since it is a simple, linear smoother, it is very interpretable and it can be used for tasks that would be intractable for the original forest. This includes bias correction, confidence intervals, assessing variable importance and methods for exploring the structure of the forest. We illustrate the method on some synthetic examples and on data related to Covid-19.

*Keywords:* Random Forest, Nonparametric regression, generalized Jackknife

# 1 Introduction

Random forests are often an accurate method for nonparametric regression but they are notoriously difficult to interpret. Also, it is difficult to construct standard errors, confidence intervals and meaningful measures of variable importance. In this paper, we construct a spatially adaptive local linear smoother that approximates the forest. Our approach builds on the ideas in Bloniarz et al. (2016) and Friedberg et al. (2020). The main difference is that we define a one parameter family of bandwidth matrices which help with the construction of confidence intervals, and measures of variable importance.

Our starting point is the well-known fact that a random forest can be regarded as a type of kernel smoother (Breiman (2000); Scornet (2016); Lin and Jeon (2006); Geurts et al. (2006); Hothorn et al. (2004); Meinshausen (2006)). We take it as a given that the forest is an accurate predictor and we do not make any attempt to improve the method. Instead, we want to find a family of linear smoothers that approximate the forest. Then we show how to use this family for interpretation, bias correction, confidence intervals, variable importance and for exploring the structure of the forest.

**Related Work.** Our work builds on Bloniarz et al. (2016) and Friedberg et al. (2020). Bloniarz et al. (2016) fit a local linear regression using weights from a random forest. They show that this often leads to improved prediction. Friedberg et al. (2020) go further and modify the forest algorithm to account for the fact that a local linear fit will be used and to reduce the bias of the fit. This further improves the performance and yields confidence intervals.

We use the forest weights to fit a local linear regression but we do so by first building a family of bandwidth matrices  $\{hH_x : h > 0, x \in \mathbb{R}^d\}$  depending on one free parameter

$h > 0$ . We use the bandwidth matrices to define a kernel from which we get the local linear fit. Creating the bandwidth matrices has several advantages. First, it allows us to use the generalized jackknife to correct the bias and construct confidence intervals. In contrast to Friedberg et al. (2020), this allows us to use any off-the-shelf random forest; no adjustments to the forest algorithm are required. Second, the collection of bandwidth matrices will be used to create several summaries of the forest. For example, we can examine how much smoothing is done with respect to different covariates and in different parts of the covariate space. We also define the notion of a typical bandwidth matrix using the Wasserstein barycenter. Third, we can explore variable importance based on local slopes at different resolutions by varying the parameter  $h$  thus giving a multiresolution measure of variable importance.

**Paper Outline.** In Section 2 we define the forest guided smoother. In Section 3 we discuss the construction of confidence intervals. In Section 4 we present methods for exploring the structure of the forest. Examples are presented in Section 5. Section 6 contains concluding remarks.

## 2 Forest-Guided Smoothers

Let

$$(X_1, Y_1), \dots, (X_n, Y_n) \sim P$$

where  $Y_i \in \mathbb{R}$  and  $X_i \in \mathbb{R}^d$ . We assume that  $d < n$  and is fixed. Let  $\mu(x) = \mathbb{E}[Y|X = x]$  denote the regression function. Recall that the random forest estimator  $\hat{\mu}_{RF}(x)$  is

$$\hat{\mu}_{RF}(x) = \frac{1}{B} \sum_{j=1}^B \hat{\mu}_j(x)$$

where each  $\hat{\mu}_j$  is a tree estimator built from a random subsample of the data, a random subsample of features and  $B$  is the number of subsamples.

We take, as a starting point, the assumption that  $\hat{\mu}_{RF}$  is a good estimator. Our goal is not to improve the random forest or provide explanations for its success. Rather, we construct an estimator that provides a tractable approximation to the forest which can then be used for other tasks.

As noted by Hothorn et al. (2004); Meinshausen (2006) the random forest estimator  $\hat{\mu}(x)_{RF}$  can be re-written as

$$\hat{\mu}_{RF}(x) = \sum_{i=1}^n w_i(x) Y_i$$

for some weights  $w_i(x)$  where  $w_i(x) \geq 0$  and  $\sum_i w_i(x) = 1$ . As these authors note, these weights behave like a spatially adaptive kernel.

We proceed as follows. As in Friedberg et al. (2020) we split the data into two groups  $D_1$  and  $D_2$ . For simplicity, assume each has size  $n$ . We construct a random forest  $\hat{\mu}_{RF}$  from  $D_1$ . Now we define the bandwidth matrix

$$H_x = \left( \frac{1}{n} \sum_i w_i(x) (X_i - x)(X_i - x)^T \right)^{1/2} \quad (1)$$

where the sum is over  $D_1$ . Let  $K$  be a spherically symmetric kernel and define

$$K(x; H_x) = |H_x|^{-1} K(H_x^{-1}x).$$

This yields a kernel centered at  $x$  whose scale matches the scale of the forest weights. We then define the one parameter family of bandwidth matrices  $\Xi = \{hH_x : h > 0, x \in \mathbb{R}^d\}$ .

We define the forest guided local linear smoother, or FGS, to be the local linear smoother  $\hat{\mu}_h(x)$  with kernel  $K(x; hH_x)$ , that is,  $\hat{\mu}_h(x) = \hat{\beta}_0(x)$  obtained by minimizing

$$\sum_i \left( Y_i - \beta_0(x) - \beta(x)^T (X_i - x) \right)^2 K(X_i - x; hH_x).$$

Then

$$\hat{\mu}_h(x) = e_1^T (X_x^T W_x X_x)^{-1} X_x W_x Y = \sum_i \ell_i(x; hH_x) Y_i$$

where

$$X_x = \begin{bmatrix} 1 & (X_1 - x)^T \\ \vdots & \vdots \\ 1 & (X_n - x)^T \end{bmatrix},$$

$W_x$  is a diagonal matrix with  $W_x(i, i) = K(X_i - x; hH_x)$ ,  $e_1 = (1, 0, \dots, 0)^T$  and

$$\ell(x; hH_x) = e_1^T (X_x^T W_x X_x)^{-1} X_x W_x. \quad (2)$$

When  $h = 1$ , which can be regarded as a default value, we write  $\hat{\mu}_h(x)$  simply as  $\hat{\mu}(x)$ . Although we focus on local linear regression, one can also use this for kernel regression or higher order local polynomial regression. We shall see that  $\hat{\mu}(x)$  is often a good approximation to  $\hat{\mu}_{RF}(x)$ .

**Remark:** Other approaches for choosing  $H_x$  are possible. For example, one could minimize the difference between  $K(x - X_i; H_x)$  and  $w_i(x)$  over all positive definite matrices  $H_x$ . However, (1) is simple and in our experience works quite well. In high dimensional cases,  $H_x$  would require regularization but we do not pursue the high dimensional case in this paper.

Figure 1 shows a one-dimensional example. The top left shows the data, the random forest estimator  $\hat{\mu}_{RF}$  in black, and the true function in red. The forest guided smoother  $\hat{\mu}(x)$  is the black line in the top right plot. The bottom left shows the weights  $w_1(x), \dots, w_n(x)$  at  $x = 0$  and the bottom right shows our kernel approximation to the weights. We see that the FGS approximates the forest and the kernel approximates the weights very well.

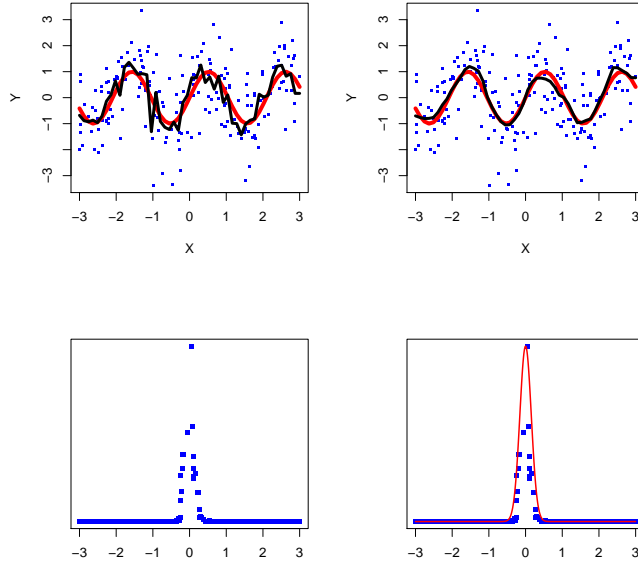


Figure 1: Top left: The data points, the random forest estimator  $\hat{\mu}_{RF}(x)$  in black, and the true function in red. Top right: forest guided smoother  $\hat{\mu}(x)$  in black, and the true function in red. Bottom left: forest weights  $w_1(x), \dots, w_n(x)$  evaluated at  $x = 0$ . Bottom right: kernel approximation to the weights.

Figure 2 shows a two-dimensional example. Here we show the forest weights as gray circles and the ellipse represents the approximating kernel. The target point is  $(0,0)$ . Again, the kernel approximates the weights.

For getting standard errors and confidence intervals, we will also need to estimate the variance

$$\sigma^2(x) = \text{Var}(Y|X = x).$$

We will proceed as follows. Let  $r_i = Y_i - \hat{\mu}_{RF}(X_i)$  be the residuals from the forest. We regress the  $r_i^2$ 's on  $X_i$ 's to estimate  $\sigma^2(x)$  using another random forest. We find that this approach tends to under-estimate  $\sigma^2(x)$  in some cases and we replace  $\hat{\sigma}(x)$  with  $c\hat{\sigma}(x)$

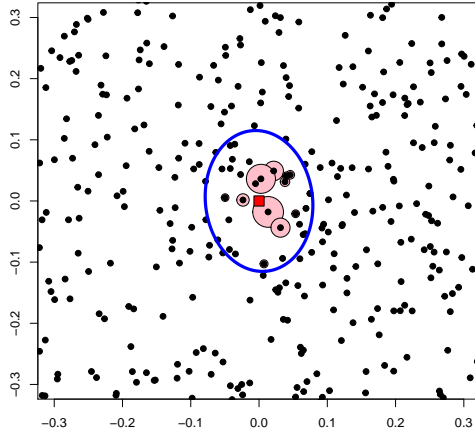


Figure 2: The dots represent data point. The target point  $x$  is indicated by the red square. The gray circles show the forest weights and the blue ellipse represents the kernel approximation to the weights.

where we use  $c = 1.5$  as a default to compensate for this in our examples.

### 3 Confidence Intervals

In this section we construct estimators of the bias of  $\hat{\mu}(x)$  and then obtain confidence intervals for  $\mu(x)$ . This is difficult to do directly from the forest without delicate modifications of the forest algorithm to undersmooth, as in Friedberg et al. (2020). But bias estimation using standard methods is possible with the FGS. We start by recalling some basic properties of local linear smoothers.

#### 3.1 Properties of Smoothers

Let  $\hat{\mu}$  be the local linear smoother based on bandwidth matrices  $H_x \equiv H_{n,x}$ . Let  $f(x)$  be the density of  $X$ , define  $\mu_2(K)$  by  $\int uu^T K(u)du = \mu_2(K)I$ , and  $R(K) = \int K^2(u)du$ . Let

Hess be the Hessian of  $\mu$ . Ruppert and Wand (1994) consider the following assumptions.

(A1)  $K$  is compactly supported and bounded. All odd moments of  $K$  vanish.

(A2)  $\sigma^2(x)$  is continuous at  $x$  and  $f$  is continuously differentiable. Also, the second order derivatives of  $\mu$  are continuous. Further,  $f(x) > 0$  and  $\sigma^2(x) > 0$ .

(A3)  $H_{n,x}$  is symmetric and positive definite. As  $n \rightarrow \infty$  we have  $n^{-1}|H_{n,x}| \rightarrow 0$  and  $H_{n,x}(i, j) \rightarrow 0$  for every  $i$  and  $j$ .

(A4) There exists  $c_\lambda$  such that

$$\frac{\lambda_{\max}(H_{n,x})}{\lambda_{\min}(H_{n,x})} \leq c_\lambda$$

for all  $n$  where  $\lambda_{\max}$  and  $\lambda_{\min}$  denote the maximum and minimum eigenvalues.

Under these conditions, Ruppert and Wand (1994) showed that the bias  $B(x, H_x)$  and variance  $V(x, H_x)$  of  $\hat{\mu}(x)$ , conditional on  $X_1, \dots, X_n$  are

$$B(x, H_x) = \frac{1}{2}\mu_2(K)\text{tr}(H_x^2\text{Hess}(x)) + o_P(\text{tr}(H_x^2)) \quad (3)$$

and

$$V(x, H_x) = \frac{\sigma^2(x)R(K)}{n|H_x|f(x)}(1 + o_P(1)). \quad (4)$$

It follows that the bias using bandwidth  $hH_x$  satisfies

$$B(x, hH_x) = h^2c_n(x) + o_P(h^2\text{tr}(H_x^2))$$

for some  $c_n(x)$ .

Assumptions (A3) and (A4) capture the idea that the bandwidth matrix needs to shrink towards 0 in some sense. Assumption (A4) essentially says that  $H_{n,x}$  behaves like a scalar

tending to 0 times a fixed positive definite matrix. For our results, we will make this more explicit and slightly strengthen (A4) to:

(A4) There exists a sequence  $\phi_n \rightarrow 0$  and a positive definite symmetric matrix  $C_x$  such that  $H_{n,x} \sim \phi_n C(x)$  where  $\phi_n \asymp (1/n)^a$  for some  $0 < a < 1$ .

With (A4) we have  $B(x, hH_x) = h^2 c(x)/n^2 + o_P(h^2)$ . To construct the bias correction we need to add the following stronger smoothness condition.

(A5) For some  $t$ , the  $t^{\text{th}}$  order derivatives of  $\mu$  are continuous and there exist functions  $c_1(x), \dots, c_t(x)$  such that, for any  $h > 0$ ,

$$B(x, hH_x) = \sum_{j=2}^t \frac{c_j(x)h^j}{n^{aj}} + o_P\left(\frac{1}{n^{at}}\right).$$

Ruppert (1997) showed how to estimate the bias of  $\hat{\mu}(x)$  by fitting the estimator for several values of the bandwidth. This type of bias estimation has been used in other contexts and is sometimes referred to as generalized jackknife; see for example Cattaneo et al. (2013).

In more detail, Ruppert's method (i.e. the generalized jackknife) works as follows. Choose a set of  $b$  bandwidths  $h_1, h_2, \dots, h_b$  and let  $\hat{m} = (\hat{\mu}_{h_1}(x), \dots, \hat{\mu}_{h_b}(x))$ . Let  $\kappa_n = (\mu(x), \kappa_{2,n}(x), \dots, \kappa_{t,n}(x))^T$  where  $\kappa_{j,n}(x) = c_j(x)/n^{ja}$ . Let

$$\mathcal{H} = \begin{bmatrix} 1 & h_1^2 & h_1^3 & \dots & h_1^t \\ 1 & h_2^2 & h_2^3 & \dots & h_2^t \\ \vdots & \vdots & \vdots & & \vdots \\ 1 & h_b^2 & h_b^4 & \dots & h_b^t \end{bmatrix}.$$

We estimate  $\kappa_n$  by least squares, namely,

$$\hat{\kappa}_n = \operatorname{argmin}_c \|\hat{m} - \mathcal{H}c\|^2 = (\mathcal{H}^T \mathcal{H})^{-1} \mathcal{H}^T \hat{m}.$$

Now  $\hat{m} = LY$  where

$$L = \begin{bmatrix} \ell_1(x; h_1 H_x) & \ell_2(x; h_1 H_x) & \dots & \ell_n(x; h_1 H_x) \\ \ell_1(x; h_2 H_x) & \ell_2(x; h_2 H_x) & \dots & \ell_n(x; h_2 H_x) \\ \vdots & \vdots & & \vdots \\ \ell_1(x; h_b H_x) & \ell_2(x; h_b H_x) & \dots & \ell_n(x; h_b H_x) \end{bmatrix}$$

where  $\ell_i(x; h_j H_x)$  are the elements of the vector  $\ell(x; h_j H_x)$  defined in (2). Therefore

$$\hat{\kappa}_n = (\mathcal{H}^T \mathcal{H})^{-1} \mathcal{H}^T L Y.$$

We estimate the bias of  $\hat{\mu}_h(x)$  by

$$\hat{B}(x, h) = \sum_{j=2}^t \hat{\kappa}_{j,n}(x) h^j = g^T (\mathcal{H}^T \mathcal{H})^{-1} \mathcal{H}^T L Y$$

where  $g = (0, h^2, \dots, h^t)^T$ . The de-biased estimator is the first element of  $\hat{\kappa}_n$ , that is,

$$\mu^\dagger(x) = e_1^T (\mathcal{H}^T \mathcal{H})^{-1} \mathcal{H}^T L Y = \sum_i \tilde{\ell}_i(x)$$

where  $\tilde{\ell}(x) = e_1^T (\mathcal{H}^T \mathcal{H})^{-1} \mathcal{H}^T L$ .

The variance of  $\mu^\dagger(x)$  (conditional on the  $X_i$ 's) is

$$\text{Var}[\mu^\dagger(x)] = \sum_i \tilde{\ell}_i^2(x) \sigma^2(X_i)$$

and the estimated variance is

$$s^2(x) = \sum_i \tilde{\ell}_i^2(x) \hat{\sigma}^2(X_i).$$

Ruppert used the bias estimation method as part of a bandwidth selection method. We are interested, instead, to get a centered central limit theorem. We now confirm that this

indeed works. For the theory, we need to be more specific about the choice of bandwidths in the bias correction procedure. Specifically, let  $h_j = \alpha_j n^{-\gamma}$ , for  $j = 1, 2, \dots, b$ , with  $0 < \alpha_1 < \dots < \alpha_b$  being constants not depending on  $n$ .

**Theorem 1** *Assume that, conditional on  $D_1$ , assumptions (A1)-(A5) hold and:*

$$(i) \quad \sup_x |\hat{\sigma}^2(x) - \sigma^2(x)| \xrightarrow{P} 0,$$

$$(ii) \quad -a < \gamma < \frac{1-ad}{d}.$$

*Further, if  $t < d/2$  we require  $a < 1/(d - 2t)$ . Also, assume that  $Y$  is bounded and that  $b > t + 1$ . Then*

$$\frac{\mu^\dagger(x) - \mu(x)}{s(x)} \rightsquigarrow N(0, 1).$$

*Hence,*

$$\mathbb{P}(\mu(x) \in C_n(x)) \rightarrow 1 - \alpha$$

*where  $C_n(x) = \mu^\dagger(x) \pm z_{\alpha/2} s(x)$ .*

The proof is in the appendix.

It is important to note that  $\gamma$  can be 0 or even negative. Ruppert (1997) requires  $\gamma > 0$ . The difference is that our bandwidth is of the form  $hH_x$  and  $H_x$  is already tending to 0 and we only need the product to go to 0. This significantly simplifies the choice of grid of bandwidths because the bandwidths can be constant order and don't need to change with  $n$ . For example, one could use a grid like  $(1/8, 1/4, 1/2, 1, 2, 4, 8)$ . We recommend including  $h = 1$  in the grid as this corresponds to the original FGS.

## 3.2 Variability Intervals

A commonly used alternative to confidence intervals for nonparametric regression is to form some sort of interval around the estimate that informally represents uncertainty but without the coverage claim of a confidence interval. We will refer to these as variability intervals. The simplest approach is to use  $\hat{\mu}(x) \pm c_\alpha s(x)$  where  $s^2(x)$  is the estimated variance of  $\hat{\mu}(x)$ . If  $\hat{\mu}(x)$  satisfies a central limit theorem and  $c_\alpha = z_{\alpha/2}$  then this is a confidence interval for  $\mathbb{E}[\hat{\mu}(x)]$ .

In our case, such a variability interval is simply  $C_n(x) = \hat{\mu}(x) \pm z_{\alpha/2} s(x)$ . The extra parameter  $h$  is not needed since we do not use the generalized jackknife to reduce the bias. However, it might be useful to construct multiresolution variability intervals at various resolutions  $h$ . This is the approach to inference recommended by Chaudhuri and Marron (2000) who refer to this as scale-space inference.

In Section 5 we illustrate this multiresolution approach for estimating the gradient as a measure of variable importance.

## 3.3 Discussion of Other Methods

Variability intervals for forests have been obtained in Mentch and Hooker (2016); Peng et al. (2019) by deriving a U-statistic based central limit theorem. Wager et al. (2014) estimate the variance of the forest using the jackknife. The advantage of these approaches is that they do not need to use sample splitting as we do.

Confidence intervals were obtained by Athey et al. (2019) and Friedberg et al. (2020). They also use data splitting. The main difference is that we leave the forest algorithm untouched and we use the generalized jackknife to reduce the bias. Instead, they modify

the construction of the forest and require that the forest is constructed to satisfy certain assumptions; specifically they require that the forest is built from subsamples of size  $s \asymp n^\beta$  where

$$\beta_{\min} = 1 - \left( 1 + \frac{d}{\pi} \frac{\log(1/\alpha)}{\log 1/(1-\alpha)} \right) < \beta < 1,$$

where  $\pi/d$  is a lower bound on the probability of splitting on a feature and each tree leaves a fraction of points  $\alpha$  on each side of every split.

The advantage of this approach is that it only requires the regression function to be Lipschitz whereas the generalized jackknife assumes that  $\mu(x)$  has at least  $t+1$  derivatives. The disadvantage is that the conditions on the construction of the forest are rather complicated and non-standard and one cannot use any off-the-shelf forest. As noted in Friedberg et al. (2020), the tuning of forest parameters in practice can be quite different than what is assumed in the theory. Our main assumption is simply that the local smoother has standard bias and variance properties.

Both approaches require assumptions and it is difficult to say that one set of assumptions is better than the other as they are quite incomparable. One is an assumption about the algorithm and the other is an assumption about the function and the bandwidth.

**Remark:** It may be the case that there are irrelevant variables. That is, we have that  $\mu(x) = \mu(x_S)$  for some subset of variables  $x_S$ . If the forest is able to discover the relevant variables, then the bandwidth matrix  $H_x$  might not shrink in the direction of the irrelevant variables. This is a good thing but, technically, the conditions (A3-A5) may be violated. However, the gradient and Hessian of  $\mu(x)$  vanish in the irrelevant directions and Theorem 1 still holds.

### 3.4 Examples of Confidence Intervals

Now we consider some examples. In each case, we use  $t = 2$ . The results using  $t = 3$  and  $t = 4$  are similar.

Figure 3 shows three, one dimensional examples. The plots on the left show the true functions in black and the average over 100 simulations of the pointwise 95 percent confidence bands in red. The plots on the right show the coverage (estimated by simulation) as a function of  $x$ . The sample size in each case is  $n = 1,000$ . The functions are  $\mu(x) = \sin(4x)$ ,  $\mu(x) = I(x > 1/2) - 1/2$  and  $\mu(x) = \sqrt{x(1-x)} \sin(2.1\pi/(x + .35))$ . The data were generated as  $Y_i = \mu(X_i) + \sigma\epsilon_i$  where  $\epsilon_i \sim N(0, 1)$ ,  $\sigma = .1, .03, .03$  in the three examples and  $X_i \sim \text{Unif}(0, 1)$ . We take the grid of bandwidths  $h_1, \dots, h_b$  to be an equally spaced grid of size 20 from  $h = .1$  to  $h = 2$ . In each case the coverage reaches its nominal value.

Next we consider some multivariate examples. The first is from Friedman and Roosen (1995) and is  $Y_i = \mu(X_i) + \sigma\epsilon$  where

$$\mu(x) = 10 \sin(\pi x_1 x_2) + 20(x_3 - 0.5)^2 + 10x_4 + 5x_5 \quad (5)$$

with  $n = 500$ ,  $\sigma = 1$  and  $X_i$  is uniform on  $[0, 1]^5$ . We take  $h$  to be in an equally spaced grid of size 20 from  $h = 1$  to  $h = 5$ . We construct 90 percent confidence intervals at 10 randomly selected points. The second example is from Friedberg et al. (2020) and is  $Y_i = \mu(X_i) + \sigma\epsilon$  where now

$$\mu(x) = \frac{10}{1 + \exp(-10(x_1 - .5))} + \frac{5}{1 + \exp(-10(x_2 - .5))} \quad (6)$$

with  $n = 500$ ,  $\sigma = 5$  and  $X_i$  is uniform on  $[0, 1]^5$ . We take  $h$  to be in an equally spaced grid of size 20 from  $h = 1$  to  $h = 30$ . We construct 90 percent confidence intervals at 10 randomly selected points.

Table 1 and 2 show coverage and average length of confidence intervals at 10 randomly

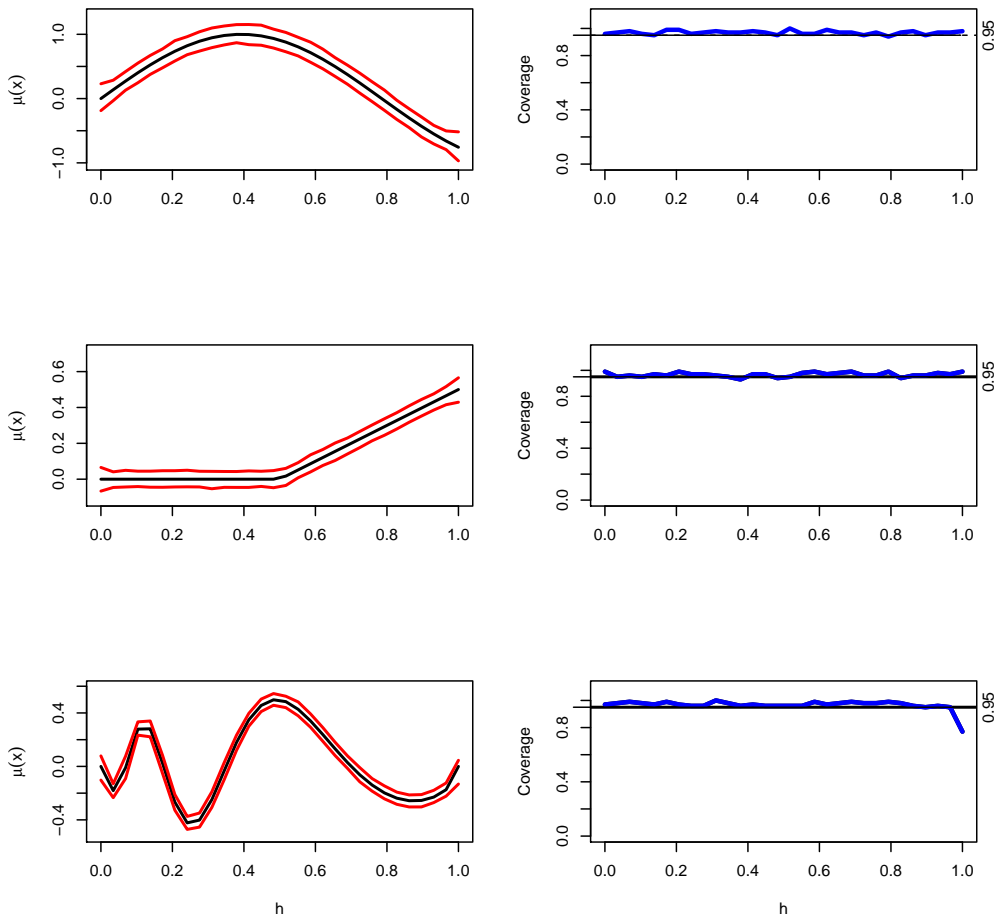


Figure 3: The figure shows three one-dimensional examples. The black lines on the left plots show the true function. The red lines on the left plots show the confidence bands from one simulation. The right plots show the estimated coverage at each  $x$  based on 100 simulations.

Table 1: Coverage and average length of confidence intervals for the function in (5)

	1	2	3	4	5	6	7	8	9	10
Coverage	0.87	0.84	0.84	0.92	0.88	0.88	0.85	0.90	0.85	0.86
Length	4.66	4.47	4.53	4.72	4.53	4.84	4.72	4.86	4.49	4.59

Table 2: Coverage and average length of confidence intervals for the function in (6)

	1	2	3	4	5	6	7	8	9	10
Coverage	0.93	0.84	0.91	0.91	0.92	0.93	0.85	0.92	0.87	0.94
Length	9.63	9.62	9.61	10.14	9.39	9.98	10.75	9.59	10.68	8.95

chosen points for the functions in (5) and (6). The coverage is close to the nominal value and the lengths are close to those in Friedman and Roosen (1995) and Friedberg et al. (2020).

**Remark.** Our grids were chosen to achieve good coverage and length for the examples. In practice we suggest a grid ranging from  $h = .1$  to  $h = 10$ . While this choice cannot be claimed to be optimal, and may not eliminate the bias, it should result in some amount of bias reduction. As pointed out in the discussion of Cattaneo et al. (2013), finding an optimal grid for the generalized jackknife is an unsolved problem.

## 4 Exploring the Forest

In this section we show how the forest guided smoother can be used to examine properties of the forest.

A random forest is a complex object and is difficult to interpret. In contrast, the FGS is completely determined by the set of bandwidth matrices  $\Xi = \{H_x : x \in \mathbb{R}^d\}$  which is a subset of the manifold of symmetric positive-definite matrices. We now consider a variety of methods for summarizing and exploring the set  $\Xi$ . In this section we describe the methods. Examples are given in Section 5.

### 4.1 Summarizing the Spatial Adaptivity of the Kernels

Here we show how to quantify the degree to which  $H_x$  varies with  $x$ . We take  $K$  to be a multivariate Gaussian. The kernel at  $x$  is  $K(x, H_x)$ . First we define what the kernel looks like on average over  $x$ . To do this we find the Wasserstein barycenter of the distributions  $\{K(0, H_x)\}$ .

The Wasserstein barycenter comes from the theory of optimal transport; a good reference on this area is Peyré and Cuturi (2019). Recall first that the (second order) Wasserstein distance between two distributions  $P_1$  and  $P_2$

$$W_2^2(P_1, P_2) = \inf_J \mathbb{E}_J[\|X - Y\|^2]$$

where  $X \sim P_1, Y \sim P_2$  and the infimum is over all joint distributions  $J$  with marginals  $P_1$  and  $P_2$ . In the special case of Normals, where  $P_1 = N(\mu_1, \Sigma_1)$  and  $P_2 = N(\mu_2, \Sigma_2)$  we have

$$W^2(P_1, P_2) = \|\mu_1 - \mu_2\|^2 + \text{tr}(\Sigma_1) + \text{tr}(\Sigma_2) - 2\text{tr}\left\{(\Sigma_1^{1/2}\Sigma_2\Sigma_1^{1/2})^{1/2}\right\}.$$

The Wasserstein barycenter of a set of distributions  $Q_x$  indexed by  $x$  is the distribution  $\bar{Q}$  that minimizes

$$\int W^2(Q_x, \bar{Q}) dP_X(x).$$

This barycenter is useful because it preserves the shape of the distributions. For example, the barycenter of a  $N(\mu_1, 1)$  and  $N(\mu_2, 1)$  is  $N((\mu_1 + \mu_2)/2, 1)$ . The Euclidean average is the mixture  $(1/2)N(\mu_1, 1) + (1/2)N(\mu_2, 1)$  which does not preserve the shape of the original densities.

In our case, we summarize the set of bandwidth matrices by finding the barycenter of the set of distributions  $\{K(0, H_{X_i})\}$ . The barycenter in this case can be shown to be  $K(0, \bar{H})$  where  $\bar{H}$  is the unique positive definite matrix such that

$$\bar{H} = \int (\bar{H}^{1/2} H_x \bar{H}^{1/2})^{1/2} dP_X(x). \quad (7)$$

In our examples, we will compute  $\bar{H}$  to see what a typical bandwidth matrix looks like. We also compute the Frechet variance

$$V = \int W^2(\bar{H}, H_x) dP_X(x)$$

which gives a sense of how much the bandwidth matrices vary over  $x$ . If  $H_x$  does not vary with  $x$  then  $V = 0$ .

Next we consider another way to summarize the FGS. For each  $X_i$ , we find the effective bandwidth with respect to each covariate by finding the length of the ellipse  $\{x : (u - X_i)^T H_{X_i}^{-1} (u - X_i) \leq c^2\}$  in the direction of each coordinate axis, for any  $c > 0$ . In other words, we compute  $\Delta_j(X_i) = \sqrt{c^2 / H_{X_i}^{-1}(j, j)}$ . In the example section we'll see that plots of these quantities can be very informative.

## 4.2 Comparing the Forest and the Smoother

How much prediction accuracy is lost by using the smoother instead of the forest? To answer this question we define

$$\Gamma = \mathbb{E}[(Y - \hat{\mu}(X))^2 - (Y - \hat{\mu}_{RF}(X))^2].$$

We can get an estimate of  $\Gamma$  using the approach in Williamson et al. (2020).

Split the data into four groups  $\mathcal{D}_1, \mathcal{D}_2, \mathcal{D}_3, \mathcal{D}_4$  each of size  $m \approx n/4$ . From  $\mathcal{D}_1$  get  $\hat{\mu}_{RF}$  and from  $\mathcal{D}_2$  get  $\hat{\mu}$ . Let

$$\hat{\Gamma} = \frac{1}{m} \sum_{i \in \mathcal{D}_3} r_i - \frac{1}{m} \sum_{i \in \mathcal{D}_4} s_i$$

where

$$r_i = (Y_i - \hat{\mu}_{RF}(X_i))^2, \quad s_i = (Y_i - \hat{\mu}(X_i))^2.$$

Then, Williamson et al. (2020) show that

$$\sqrt{m}(\hat{\Gamma} - \Gamma) \rightsquigarrow N(0, \tau^2)$$

and a consistent estimate of  $\tau^2$  is  $m^{-1}(\sum_i (r_i - \bar{r})^2 + \sum_i (s_i - \bar{s})^2)$ . Hence, a  $1 - \alpha$  confidence interval for  $\Gamma$  is  $\hat{\Gamma} \pm z_{\alpha/2} \hat{\tau} / \sqrt{m}$ . (One can repeat this by permuting the blocks and averaging if desired.)

## 4.3 Multiresolution Local Variable Importance

One popular method of assessing local variable importance is to estimate the gradient of  $\hat{\mu}$  or, equivalently, to use local linear approximations Ribeiro et al. (2016); Plumb et al. (2018). Using the forest guided local linear smoother we get an estimate of the gradient and

its standard error for free. Furthermore, we can do this at various resolutions by varying  $h$ .

Let  $\hat{\beta}_h(x) = (\hat{\beta}_{h,1}(x), \dots, \hat{\beta}_{h,d}(x))$ . Now

$$\hat{\beta}_{h,j}(x) = \sum_i Y_i \ell_{ij}(x; hH_x)$$

where  $\ell_{ij}(x; hH_x)$  is the  $i^{\text{th}}$  element of the vector

$$e_{j+1}^T (X_x^T W_x X_x)^{-1} X_x W_x,$$

where  $W_x$  is a diagonal matrix with  $W_x(i, i) = K(X_i - x; hH_x)$  and  $e_{j+1}$  is the vector that is all 0 except it is 1 in the  $j + 1$  position. The standard error of  $\hat{\beta}_{j,h}(x)$  is  $\text{se}_{j,h}(x) = \sqrt{\sum_i \hat{\sigma}^2(X_i) \ell_{ij}^2(x; hH_x)}$ . A  $1 - \alpha$  variability interval is  $\hat{\beta}_{j,h}(x) \pm z_{\alpha/2} \text{se}_{j,h}(x)$ .

A plot of the values  $\hat{\beta}_{h,j}(X_i)$  gives a global sense of the local importance of the  $j^{\text{th}}$  covariate. A plot of  $\hat{\beta}_{h,j}(x)$  as a function of  $h$  for a fixed  $x$  summarizes local variable importance at various resolutions.

## 5 Examples

In this section, we illustrate the methods from the previous section on two examples. The first is a synthetic example and the second is a data example.

### 5.1 Synthetic Example

We return to the example given in (6). Figure 4 shows the Wasserstein barycenter of the bandwidth matrices. The barycenter shows that the typical bandwidth for the first two variables is small. This makes sense as the function only depends on  $x_1$  and  $x_2$ . Also, the small off-diagonals suggest the bandwidth matrix is typically not far from diagonal.

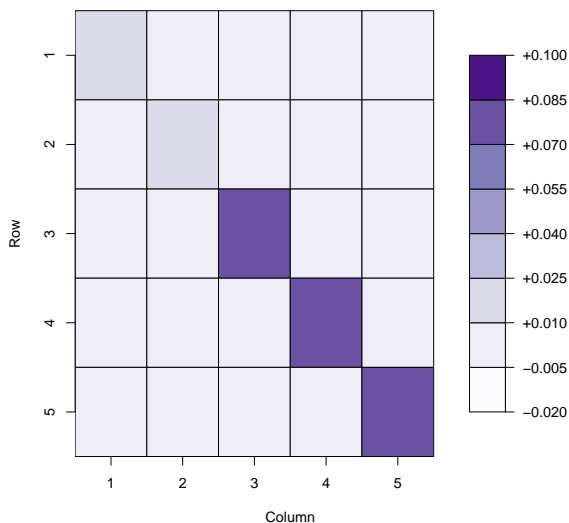


Figure 4: Barycenter of the bandwidth matrices for the example in equation (6).

The Frechet variance is 0.019, suggesting that the bandwidth matrix does not vary greatly across the sample space.

Figure 5 shows violin plots of effective bandwidths. The effective bandwidth  $\Delta_j$  is smaller for  $x_1$  and  $x_2$  than for the other variables. This is what we would expect since  $\mu(x)$  does not depend on  $x_3, x_4$  or  $x_5$ . The forest attempts to smooth over these irrelevant variables and hence the approximating bandwidth matrices tend to be large in the directions of the irrelevant variables. This confirms what we found with the barycenter.

The four plots in Figure 6 show the local slopes  $\hat{\beta}_1(X_i), \dots, \hat{\beta}_5(X_i)$  for each of the five covariates (over all  $X_i$ ) at four different resolutions. and variable importance (bottom) at several resolutions  $h = 0.1, 0.5, 1$  and  $2$ . The two smallest resolutions ( $h = 0.1, h = 0.5$ ) are uninformative. The two larger resolutions ( $h = 1, h = 2$ ) provide clear evidence of the

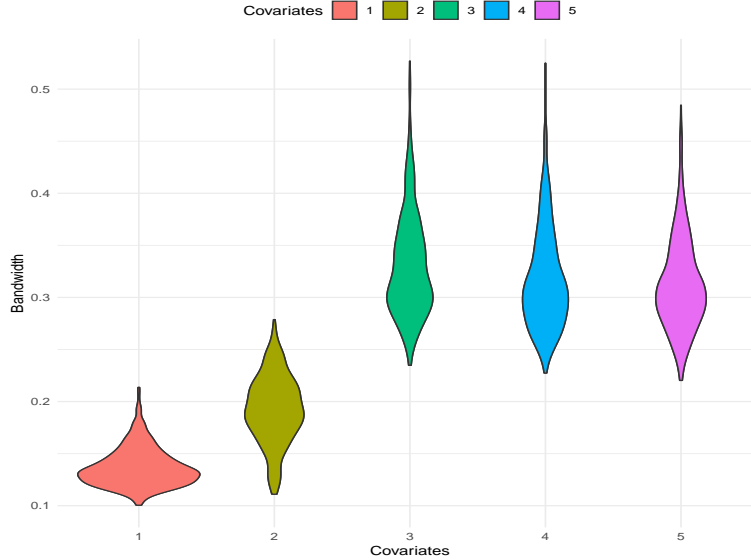


Figure 5: Example (6). Effective bandwidths for each covariate.

importance of  $x_1$  and  $x_2$ . Note that importance variables correspond to small bandwidths but large slopes.

Figure 7 shows variability intervals for  $\hat{\beta}_{1,h}(x), \dots, \hat{\beta}_{4,h}(x)$  at  $x = (1/2, 1/2, 1/2, 1/2, 1/2)$ , the center of the support of  $X$ . (The fifth variable is not shown.) These intervals are plotted versus increasing values of  $h$  resulting in (pointwise) variability bands for  $\beta_{j,h}(x)$ .

Again, we see that  $x_1$  and  $x_2$  are the important variables as the bands exclude 0 for larger values of  $h$  while the bands for  $x_3$  and  $x_4$  include 0 for all  $h$ .

Next we compare the FGS to the forest. The top left plot of Figure 8 shows histograms of the squared residuals for the forest and of the FGS. The two histograms are very similar. It also shows two scatterplots of  $\hat{\mu}_{RF}(X_i)$  and  $e\hat{\mu}(X_i)$ . and of their residuals.

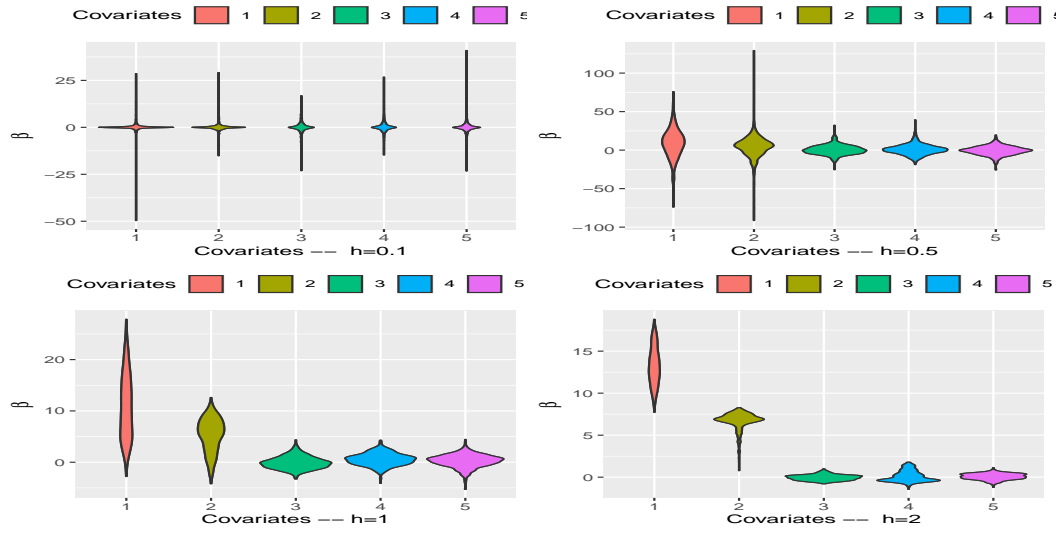


Figure 6:  $\{\hat{\beta}_j(X_1), \dots, \hat{\beta}_j(X_n)\}$  for each covariate at four resolutions,  $h = 0.1, 0.5, 1, 2$ .

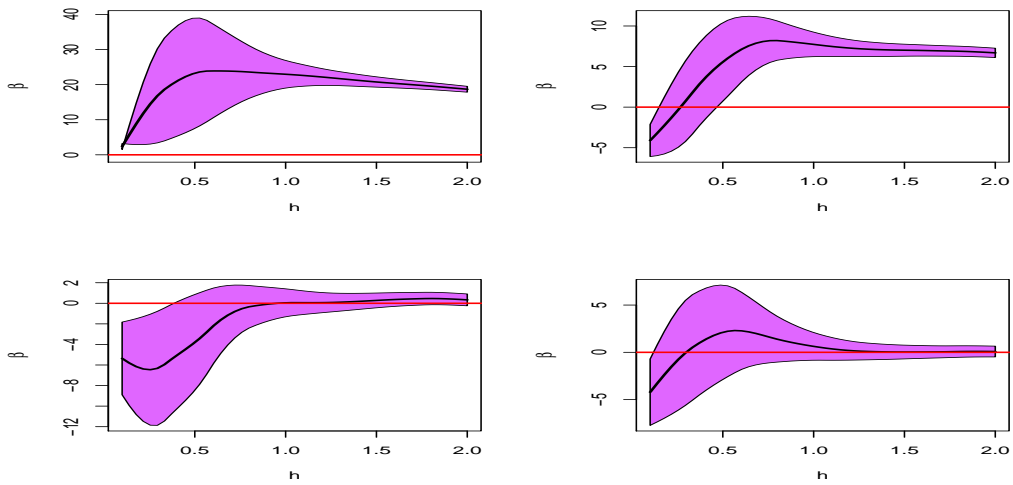


Figure 7: Variability intervals for  $\hat{\beta}_{1,h}(x), \dots, \hat{\beta}_{4,h}(x)$  at  $x = (1/2, 1/2, 1/2, 1/2, 1/2)$ .

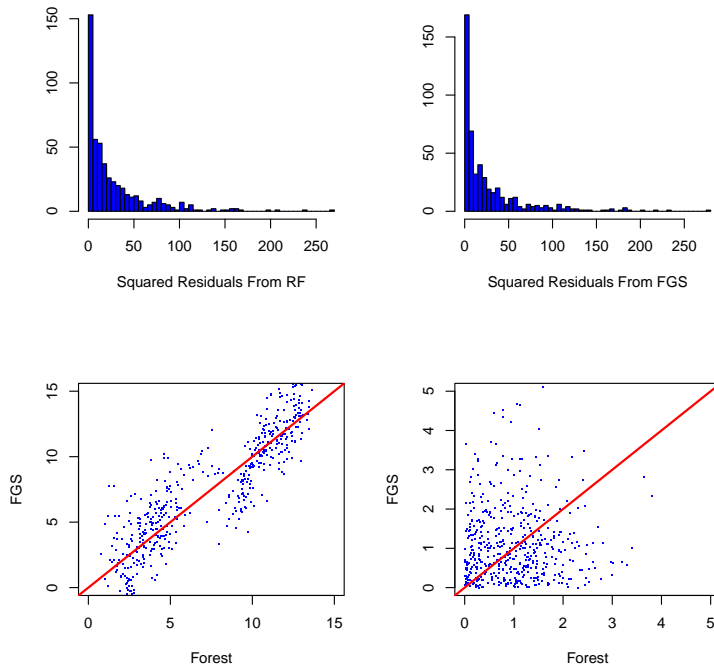


Figure 8: Top left: squared residuals from the random forest. Top right: squared residuals from the FGS. Bottom left: Plot of  $\hat{\mu}_{RF}(X_i)$  versus  $\hat{\mu}(X_i)$ . Bottom right: Plot of  $|Y_i - \hat{\mu}_{RF}(X_i)|$  versus  $|Y_i - \hat{\mu}(X_i)|$ .

We do see a very slight loss in accuracy for the FGS but the difference is small. It appears that the two fits are very similar. To formalize this, we estimate  $\Gamma$  as described in Section 4.2 and we find that the 95 per cent confidence interval  $\hat{\Gamma} = -0.134 \pm 4.9$  again suggesting little difference between the two methods. Thus we conclude that the FGS appears to be a good approximation to the forest.

## 5.2 Covid-19

In this section we consider data on Covid-19 obtained from the API of the CMU Delphi group at `covidcast.cmu.edu`.

Our goal is to construct a random forest to predict  $Y =$  average daily deaths from these variables:

cli	Percentage of people with Covid-like symptoms (surveys of Facebook users)
dr	Percentage of daily doctor visits that are due to Covid-like symptoms
cases	Newly reported Covid-19 cases per 100,000 people
home	Proportion of people staying home
masks	Percentage of people who say they wear a mask in public
hospital	Percentage of daily hospital admissions with Covid-19
prevdeaths	Previous number of deaths due to Covid-19

The variable  $Y$  is averaged over December 1 2020 to December 12 2020. The covariates are averaged from October 1 2020 to December 1 2020. We took the logarithms of all variables and then scaled each covariate to have mean 0 and variance 1.

The problem of predicting the epidemic is an intensely studied issue and our goal is not to develop a cutting edge prediction method. Rather, we use these data as a vehicle for illustrating our methods.

After fitting the FGS we can summarize the local fit for various counties by reporting the local slopes  $\hat{\beta}_1(x), \dots, \hat{\beta}_d(x)$  and their standard errors. Table 1 and Table 2, below show this for four counties. The nice thing about the FGS is that we can describe the model for any county in the familiar form of a (local) linear model. This makes the model very interpretable for users such as public health officials.

**New York County, NY**

Coefficients	$\hat{\beta}$	Standard Error
cli	-0.026	0.057
dr	-0.042	0.034
cases	-0.012	0.044
home	0.148	0.056
masks	-0.016	0.042
hospital	0.003	0.058
prevdeaths	0.128	0.082

**Elkhart County, IN**

Coefficients	$\hat{\beta}$	Standard Error
cli	0.015	0.119
dr	0.155	0.148
cases	-0.150	0.106
home	0.204	0.159
masks	0.124	0.118
hospital	-0.158	0.098
prevdeaths	0.141	0.087

**Table 3****DuPage County, IL**

Coefficients	$\hat{\beta}$	Standard Error
cli	0.62	0.077
dr	0.032	0.049
cases	-0.029	0.063
home	-0.006	0.089
masks	0.013	0.083
hospital	-0.061	0.100
prevdeaths	0.211	0.069

**Lubbock County, TX**

Coefficients	$\hat{\beta}$	Standard Error
cli	0.043	0.094
dr	0.110	0.097
cases	-0.066	0.080
home	0.105	0.108
masks	0.063	0.072
hospital	-0.065	0.061
prevdeaths	0.107	0.074

**Table 4**

Figure 9 shows the effective bandwidths and local slopes at resolution  $h = 2$ . The two most important variables (small bandwidths and large slopes) are  $x_4$  (home) and  $x_7$  (previous deaths). The importance of previous deaths is obvious. The fact that social mobility (home) is important is notable but we should emphasize that this is a predictive analysis not a causal analysis.

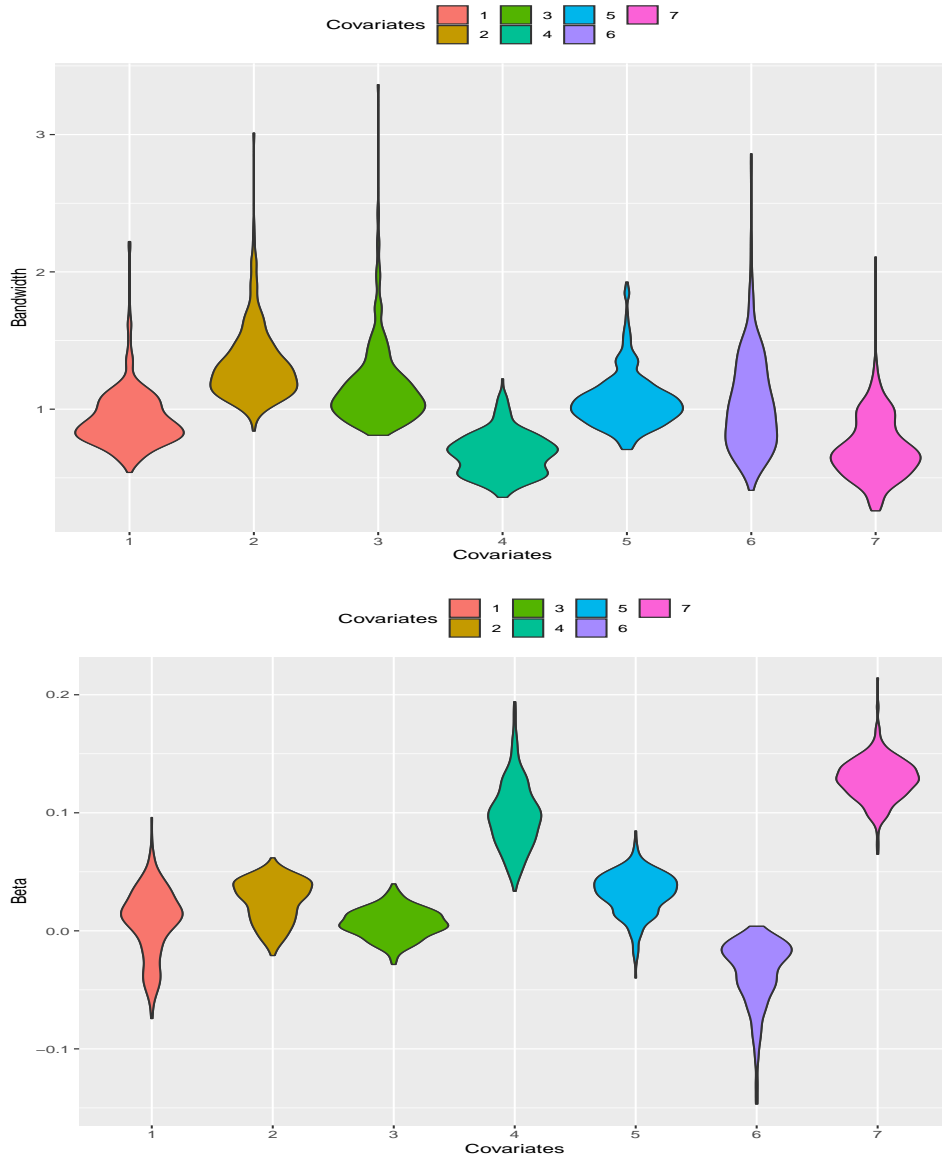


Figure 9: Bandwidth plot (top) and  $\beta$  plot (bottom) for Covid example

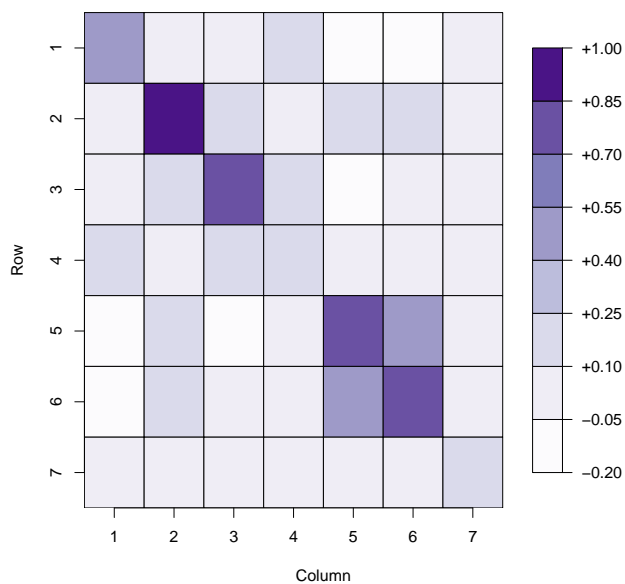


Figure 10: Barycenter of the bandwidth matrices for Covid example.

Figure 10 shows the barycenter of the bandwidth matrices. Note that the fourth and seventh elements on the diagonal are the smallest confirming the importance of those variables. We also see some correlation between the bandwidths for  $x_5$  and  $x_6$ . The Frechet variance is 0.817 suggesting that  $H_x$  varies quite a bit with  $x$  (recall that all the variables are scaled to have variance 1).

## 6 Discussion

Throughout this paper we have assumed that the number of covariates  $d$  is fixed. If  $d$  increases with  $n$  then local linear fitting will not work. Instead one will need to include

some sort of ridge or  $\ell_1$  penalty. Furthermore, when  $d$  is large,  $H_x$  will not be invertible and so regularization on  $H_x$  is required.

We have focused on random forests but similar ideas can be used for other black box methods such as neural nets. Koh and Liang (2017) show how to compute the influence function for deep nets and other predictors. The influence function can be used to define a spatially adaptive kernel as we have done using the weights from a forest.

In our examples we have not found much difference between the forest and the FGS. But this may be due to the fact that we have not considered complex high dimensional problems. Understanding when a complex predictor can be approximated by a spatially varying local smoother is an interesting but challenging problem.

## References

- Susan Athey, Julie Tibshirani, Stefan Wager, et al. Generalized random forests. *The Annals of Statistics*, 47(2):1148–1178, 2019.
- Adam Bloniarz, Ameet Talwalkar, Bin Yu, and Christopher Wu. Supervised neighborhoods for distributed nonparametric regression. In *Artificial Intelligence and Statistics*, pages 1450–1459, 2016.
- Leo Breiman. Randomizing outputs to increase prediction accuracy. *Machine Learning*, 40(3):229–242, 2000.
- Matias D Cattaneo, Richard K Crump, and Michael Jansson. Generalized jackknife estimators of weighted average derivatives. *Journal of the American Statistical Association*, 108(504):1243–1256, 2013.

- Probal Chaudhuri and James Steven Marron. Scale space view of curve estimation. *Annals of Statistics*, pages 408–428, 2000.
- Rina Friedberg, Julie Tibshirani, Susan Athey, and Stefan Wager. Local linear forests. *Journal of Computational and Graphical Statistics*, pages 1–15, 2020.
- Jerome H Friedman and Charles B Roosen. An introduction to multivariate adaptive regression splines, 1995.
- Pierre Geurts, Damien Ernst, and Louis Wehenkel. Extremely randomized trees. *Machine learning*, 63(1):3–42, 2006.
- Torsten Hothorn, Berthold Lausen, Axel Benner, and Martin Radespiel-Tröger. Bagging survival trees. *Statistics in medicine*, 23(1):77–91, 2004.
- Pang Wei Koh and Percy Liang. Understanding black-box predictions via influence functions. *arXiv preprint arXiv:1703.04730*, 2017.
- Yi Lin and Yongho Jeon. Random forests and adaptive nearest neighbors. *Journal of the American Statistical Association*, 101(474):578–590, 2006.
- Nicolai Meinshausen. Quantile regression forests. *Journal of Machine Learning Research*, 7(Jun):983–999, 2006.
- Lucas Mentch and Giles Hooker. Quantifying uncertainty in random forests via confidence intervals and hypothesis tests. *The Journal of Machine Learning Research*, 17(1):841–881, 2016.

- Wei Peng, Tim Coleman, and Lucas Mentch. Asymptotic distributions and rates of convergence for random forests via generalized u-statistics. *arXiv preprint arXiv:1905.10651*, 2019.
- Gregory Plumb, Denali Molitor, and Ameet S Talwalkar. Model agnostic supervised local explanations. In *Advances in Neural Information Processing Systems*, pages 2515–2524, 2018.
- Marco Tulio Ribeiro, Sameer Singh, and Carlos Guestrin. ” why should i trust you?” explaining the predictions of any classifier. In *Proceedings of the 22nd ACM SIGKDD international conference on knowledge discovery and data mining*, pages 1135–1144, 2016.
- David Ruppert. Empirical-bias bandwidths for local polynomial nonparametric regression and density estimation. *Journal of the American Statistical Association*, 92(439):1049–1062, 1997.
- David Ruppert and Matthew P Wand. Multivariate locally weighted least squares regression. *The annals of statistics*, pages 1346–1370, 1994.
- Erwan Scornet. Random forests and kernel methods. *IEEE Transactions on Information Theory*, 62(3):1485–1500, 2016.
- Stefan Wager, Trevor Hastie, and Bradley Efron. Confidence intervals for random forests: The jackknife and the infinitesimal jackknife. *The Journal of Machine Learning Research*, 15(1):1625–1651, 2014.
- Brian D Williamson, Peter B Gilbert, Noah R Simon, and Marco Carone. A unified approach for inference on algorithm-agnostic variable importance. *arXiv preprint arXiv:2004.03683*, 2020.

# Appendix

Here we recall Theorem 1 and give an outline of the proof.

**Theorem 3.1** Assume that (i)  $\sup_x |\hat{\sigma}^2(x) - \sigma^2(x)| \xrightarrow{P} 0$ , (ii)  $\sigma^2(x) > 0$ ,

$$(iii) \quad -a < \gamma < \frac{1-ad}{d}$$

and further, if  $t < d/2$  we require  $a < 1/(d-2t)$ . Also, assume that  $Y$  is bounded and that  $b > t + 1$ . Then

$$\frac{\mu^\dagger(x) - \mu(x)}{\sqrt{\hat{\text{Var}}[\mu^\dagger(x)]}} \rightsquigarrow N(0, 1).$$

**PROOF OUTLINE.** First note that the condition  $\gamma > -a$  ensures that  $n|hH_x| \rightarrow \infty$  and this implies  $\text{Var}[\mu^\dagger(x)] \rightarrow 0$ . We write

$$\frac{\mu^\dagger(x) - \mu(x)}{\sqrt{\text{Var}(\mu^\dagger(x))}} = \frac{\mu^\dagger(x) - \mathbb{E}[\mu^\dagger(x)]}{\sqrt{\text{Var}(\mu^\dagger(x))}} + \frac{\mathbb{E}[\mu^\dagger(x)] - \mu(x)}{\sqrt{\text{Var}(\mu^\dagger(x))}}.$$

Recall that  $\mu^\dagger(x) = e_1^T (\mathcal{H}^T \mathcal{H})^{-1} \mathcal{H}^T \hat{m}$  where  $\hat{m} = (\hat{\mu}(x; h_1 H_x), \dots, \hat{\mu}(x; h_b H_x))^T$ . Now  $\mathbb{E}[\hat{m}] = \mathcal{H}\kappa_n(x) + o(n^{-at})$  where we recall that

$$\kappa_n(x) = \left( \mu(x), \sum_{j=2}^t c_j(x) h_1^j / n^{aj}, \dots, \sum_{j=2}^t c_j(x) h_b^j / n^{ja} \right)^T.$$

Hence,

$$\mathbb{E}[\mu^\dagger(x) - \mu(x)] = e_1^T (\mathcal{H}^T \mathcal{H})^{-1} \mathcal{H}^T [\mathcal{H}\kappa_n(x) + o(n^{-at})] = o(n^{-at}).$$

Let  $\mathcal{V}$  be the covariance matrix of  $\hat{m}$ . Then, arguing as in the proof of Theorem 2.1 of Ruppert and Wand (1994), there exists a  $b \times b$  positive definite matrix  $A$  depending on  $K, \alpha_1, \dots, \alpha_b, x, f(x)$  and  $\sigma^2(x)$  but not on  $n$ , such that

$$\mathcal{V} = \frac{A}{n|h_1 H_x|} (1 + o_P(1)).$$

Hence,

$$\begin{aligned}
\text{Var}[\mu^\dagger(x)] &= e_1^T (\mathcal{H}^T \mathcal{H})^{-1} \mathcal{H}^T \mathcal{V} \mathcal{H} (\mathcal{H}^T \mathcal{H})^{-1} e_1 \\
&= \frac{1}{n|h_1 H_x|} e_1^T (\mathcal{H}^T \mathcal{H})^{-1} e_1 (1 + o_P(1)) \\
&= \frac{1}{n|h_1 H_x|} (1 + o_P(1)) \\
&= O_P(n^{1-d(a+\gamma)})
\end{aligned}$$

since  $e_1^T (\mathcal{H}^T \mathcal{H})^{-1} e_1 = O(1)$ . Since  $\gamma < (1 - ad)/d \leq \min\{(1 - ad)/d, (2at - da + 1)/d\}$  it follows that

$$\frac{\mathbb{E}[\mu^\dagger(x)] - \mu(x)}{\sqrt{\text{Var}(\mu^\dagger(x))}} = o_P(1).$$

Now  $\mathbb{E}[|\mu^\dagger(x) - \mathbb{E}[\mu^\dagger(x)]|^3] = O(n^{2d(a+\gamma)-2})$ . Hence

$$\frac{\mathbb{E}[|\mu^\dagger(x) - \mathbb{E}[\mu^\dagger(x)]|^3]}{\text{Var}[\mu^\dagger(x)]^{3/2}} = O(n^{2d(a+\gamma)-2} n^{(3/2)(1-d(a+\gamma))}) = o_P(1)$$

since  $\gamma < (1 - ad)/d$ . Hence, by Lyapunov's central limit theorem,

$$\frac{\mu^\dagger(x) - \mathbb{E}[\mu^\dagger(x)]}{\sqrt{\text{Var}(\mu^\dagger(x))}} \rightsquigarrow N(0, 1).$$

Finally, since  $\sup_x |\hat{\sigma}^2(x) - \sigma^2(x)| \xrightarrow{P} 0$  and  $\sigma^2(x) > 0$ , it follows that  $\hat{\text{Var}}[\mu^\dagger(x)]/\text{Var}[\mu^\dagger(x)] \xrightarrow{P} 1$  and the result follows.